SUPPORTING INFORMATION

Theoretical Kinetic Study of the Formic Acid Catalyzed Criegee Intermediate Isomerization: Multistructural Anharmonicity and Atmospheric Implications

Manuel Monge-Palacios,[1*] Matti P. Rissanen,[2] Zhandong Wang[1] and S. Mani Sarathy[1]

1. Conformational Analysis of the Reactant C6-CI and Saddle Point. The different ways the low- and high-energy conformers of the reactant C6-CI and saddle point are folded is exemplified. Figures S1 and S2 show the ωB97X-D/6-311+G(d,p) optimized structures of two low-energy, (a) and (b), and two high-energy, (c) and (d), conformers of C6-CI and saddle point, respectively. As for the reactant C6-CI (Figure S1), the CCSD(T)/6-311+G(d,p)//ωB97X-D/6-311+G(d,p) energies (without the ZPE correction and defined with respect to the energy of the global minimum) of the conformers (a), (b), (c) and (d) are 0.35, 0.47, 3.62 and 3.74 kcal mol^{-1}, respectively. The bent structure of (a) and (b) induces the formation of the C(4)–H(6)···O(19) and C(7)–H(9)···O(1) hydrogen bonds by approaching oxygen and hydrogen atoms that are distant in the chain. This is not possible in the conformers (c) and (d), with a more elongated structure.

Figure S2 shows the same results for the saddle point; the energies of the conformers (a), (b), (c) and (d) are 0.20, 0.90, 4.57 and 6.53 kcal mol^{-1}, respectively. In these structures the terminal atom O(1) plays a role in the formation of the C(7)–H(9)···O(1) and C(10)–H(12)···O(1) hydrogen bonds, stabilizing the conformers (a) and (b). However, this is not the case with conformers (c) and (d), in which the O(1) atom is further away from the hydrogen atoms of the chain. In the saddle point the O(19) atom is not available for the formation of additional hydrogen bonds as occurs in C6-CI because it is involved in the double hydrogen transfer reaction. This results in fewer hydrogen bonds than in the case of the conformers of the reactant C6-CI. In addition, in the saddle point there are likely steric effects between the carbon chain of the C6-CI fragment, which tends to be folded, and the HCOOH fragment, which must be kept in a very specific position to ensure that the angles O(22)–H(23)–O(19) and O(24)–H(14/15)–O(13) are collinear to facilitate the simultaneous transfer of two hydrogen atoms. As a result, the conformers of the reactant C6-CI

[1] King Abdullah University of Science and Technology, Clean Combustion Research Center, Thuwal 23955-6900, Saudi Arabia.
[2] Department of Physics, University of Helsinki, P. O. Box 64, Helsinki, 00014, Finland.
Corresponding author's e-mail address: manuel.mongepalaciosm@kaust.edu.sa

are more numerous and closer in energy to their global minimum than those of the saddle point. Both factors, number and stability of the conformers, determine the multistructural anharmonicity, as will be discussed in the next Section.

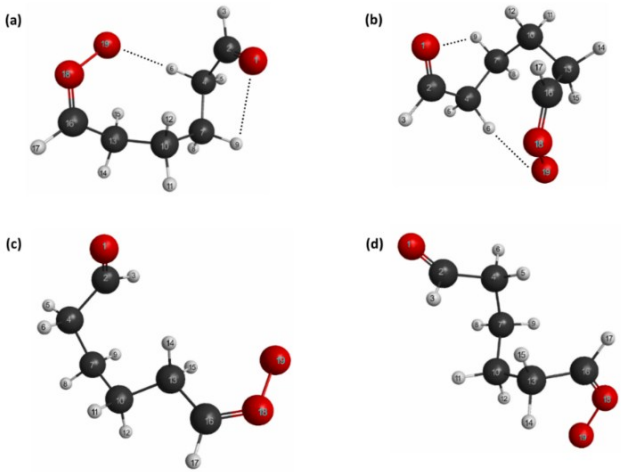

Figure S1. Optimized structures at the ωB97X-D/6-311+G(d,p) level of four of the conformers of the reactant C6-CI.

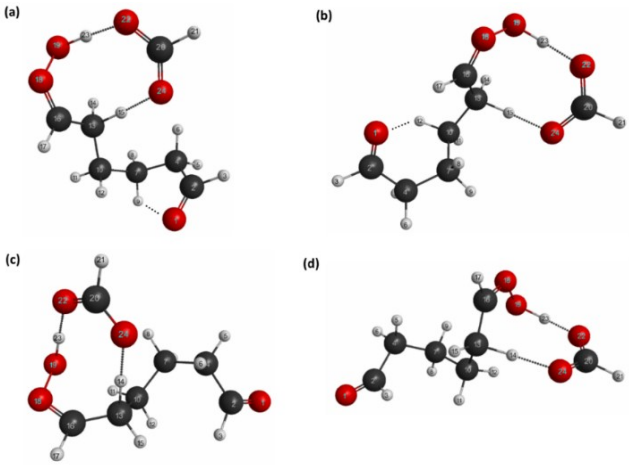

Figure S2. Optimized structures at the ωB97X-D/6-311+G(d,p) level of four of the conformers of the saddle point.

2. Analysis of the Multistructural Anharmonicity. The aforementioned differences in the number and relative stability of the conformers of C6-CI and saddle point make those of C6-CI have a significant contribution to the multistructural partition function $Q_{con-rovib}^{MS-T(C)}$ (Eq. 2). Thus,

the multistructural anharmonicity factor of C6-CI ($F^{MS-T(C)}_{C6-CI}$) is much larger than that of the saddle point, leading to total factors $F^{MS-T(C)}$ lower than 1.0 and hindering the reactivity. The calculated multistructural anharmonicity factors for the reactants, saddle point and for the reaction are given in Table S1; its variation with temperature is shown in Figure S3. The total multistructural anharmonicity factor significantly changes in the temperature range of atmospheric interest, highlighting the importance of considering the effect of the multistructural anharmonicity for a better description of the kinetics of these complex reactions, as well as their implication in atmospheric chemistry. However, this can be computationally prohibitive in large reactive systems for which extensive electronic structure calculations are necessary. The studied reaction can be used to model more complex systems with structural similarities, helping to overcome this drawback.

Table S1. Multistructural torsional anharmonicity factors with a coupled torsional potential (unitless) for the reactants, saddle point and total.

T (K)	$F^{MS-T(C)}_{C6-CI}$	$F^{MS-T(C)}_{HCOOH}$	$F^{MS-T(C)}_{SP}$	$F^{MS-T(C)}$
230	63.47	1.00	21.21	0.33
240	68.33	1.00	22.47	0.33
250	73.51	1.00	23.83	0.32
260	79.01	1.00	25.29	0.32
270	84.80	1.00	26.84	0.32
280	90.88	1.00	28.49	0.31
290	97.22	1.00	30.23	0.31
298	102.48	1.00	31.69	0.31
310	110.65	1.00	33.99	0.31
320	117.71	1.00	36.01	0.31
350	140.08	1.00	42.60	0.30
400	180.41	1.00	55.34	0.31
500	266.43	1.01	86.83	0.32
600	350.97	1.03	125.02	0.35
800	494.72	1.08	213.72	0.40
1000	597.18	1.13	306.87	0.45
1200	663.79	1.20	394.76	0.50
1600	723.06	1.31	538.96	0.57
2000	725.72	1.41	639.58	0.62

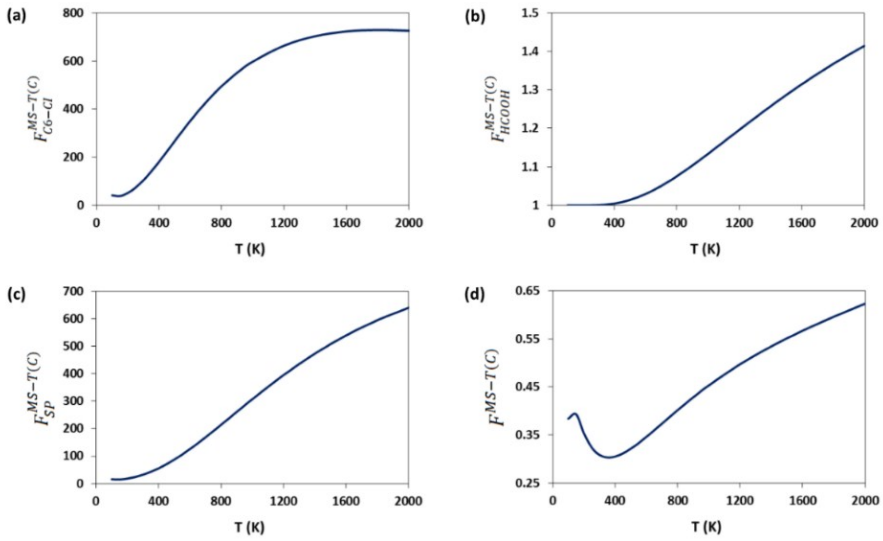

Figure S3. Multistructural torsional anharmonicity factors with a coupled torsional potential (unitless) as function of temperature for the reactants (a, b), saddle point (c) and total (d).

The value of the singlestructural rotational-vibrational partition function ($Q_{con-rovib,j}^{SS-T(C)}$) of the conformers of the reactant and saddle point is shown in Figures S4a and S4b (solid line, left y-axis), respectively, at 298 K. The conformers are represented in the x-axis by their *j* labels. The potential energy (without the ZPE correction) of the conformers is also plotted (dashed line, right y-axis). Thus, this figure displays the contribution of each conformer to the total conformational rotational-vibrational partition function ($Q_{con-rovib}^{MS-T(C)}$) at 298 K, and thereby to the total multistructural torsional anharmonicity factor ($F^{MS-T(C)}$) at that temperature, as function of its potential energy. For instance, 40 conformers ($j \leq 40$) of the reactant C6-CI have an energy equal or lower to 2.0 kcal mol^{-1} with respect to that of the global minimum ($j = 0$, E = 0.0 kcal mol^{-1}), thus showing each one a large value of $Q_{con-rovib,j}^{SS-T(C)}$ and a large contribution to $F^{MS-T(C)}$. This is not the case of the saddle point, which only has 8 conformers within that energy range and shows a quick decay of the value of $Q_{con-rovib,j}^{SS-T(C)}$ as energy increases.

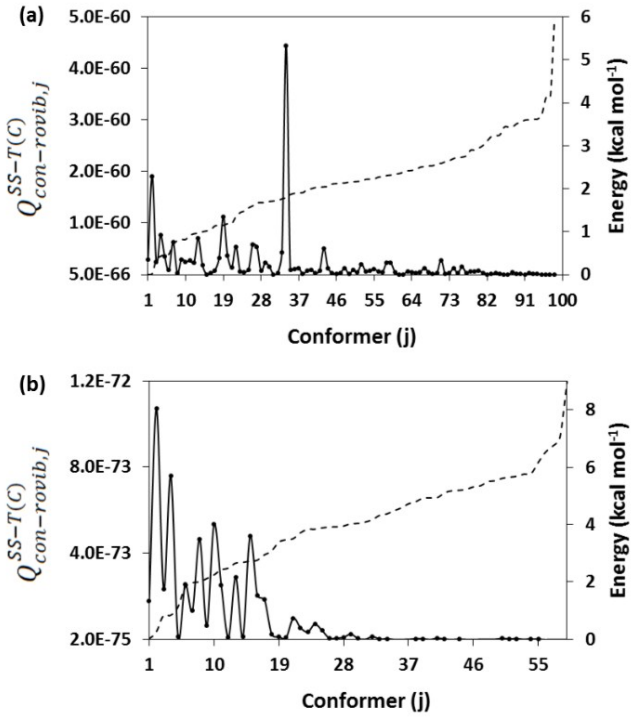

Figure S4. Values of the singlestructural rotational-vibrational partition function (solid line, left y-axis) at 298 K and potential energy (dashed line, right y-axis) of the conformers of the reactant C6-CI (a) and saddle point (b). The conformers are represented in the x-axis by their *j* labels.

Figure S4a also shows that the conformer $j = 34$ of the reactant C6-CI, with a potential energy of around 1.79 kcal mol^{-1} with respect to that of the global minimum, is the one that contributes in the largest extent to $Q_{con-rovib}^{MS-T(C)}$, despite not being the global potential energy minimum. This is because in the lower potential energy conformers ($j < 34$) the hydrogen bonds also contribute to increase their free energy by reducing the entropy, thereby lowering their contribution to $Q_{con-rovib}^{MS-T(C)}$. This also applies to the conformer $j = 2$ of the saddle point (Figure S4b).